

Nikola MIŠKOVIĆ
Đula NAĐ
Zoran VUKIĆ

3D Line Following for Unmanned Underwater Vehicles

Original scientific paper

When designing guidance controllers for unmanned underwater vehicles, an assumption is often made that the vessel operates at a constant depth. However, in many applications the desired depth often changes with the position of the vessel in the horizontal plane. This paper addresses the problem of three dimensional line following with the application to underactuated underwater vehicles. The problem is resolved by separating the desired line into two components. The main contribution of this paper is the design of 3D line following controllers for underactuated underwater vehicles. The control design is based on constant controlled surge speed and a simplified decoupled model of an underwater vehicle. Detailed design procedure is presented. The simulation results are obtained from a complex, coupled model, which proves that the proposed algorithm can be used on real vehicles.

Keywords: control, line following, marine vehicles, unmanned underwater vehicles

Praćenje 3D pravca za bespilotne ronilice

Izvorni znanstveni rad

Prigodom projektiranja sustava vođenja za bespilotne ronilice često se pretpostavlja da plovilo radi na stalnoj dubini. No, u mnogim se primjenama željena dubina često mijenja s položajem plovila u horizontalnoj ravnini. Ovaj se članak bavi problemom praćenja pravca u tri dimenzije s primjenom na podakuirane ronilice. Problem je riješen rastavljanjem željenog pravca na dvije sastavnice. Glavni doprinos ovog članka je projektiranje regulatorâ za praćenje 3D pravca za podakuirane ronilice. Projektiranje se upravljanja temelji na konstantnoj unaprijednoj brzini i pojednostavljenom nespregnutom modelu ronilice. Predstavljen je iscrpan postupak projektiranja upravljanja. Simulacijski rezultati dobiveni su na složenom, sprengnutom modelu, što dokazuje da se predloženi algoritam može primijeniti na stvarna plovila.

Ključne riječi: bespilotne ronilice, plovila, praćenje pravca, upravljanje

Authors' Address (Adresa autora):

Laboratory for Underwater Systems and Technologies, Faculty of Electrical Engineering and Computing, University of Zagreb, Unska 3, 10000, Croatia
 E-mail: (nikola.miskovic, dula.nad, zoran.vukic)@fer.hr

Received (Primljeno): 2010-02-01

Accepted (Prihvaćeno): 2010-02-10

Open for discussion (Otvoreno za raspravu): 2011-06-30

1 Introduction

The problem of control and guidance of marine vehicles (surface and underwater) is a challenging task. The main reasons for this are the couplings between the motions, hydrodynamic effects and highly unpredictable environmental influences. Underwater marine vehicles have the greatest problem of coupling effects due to their ability to operate in a three dimensional space.

The general control structure for marine vehicles can be described with three levels of control. Low control level is in charge of controlling vehicle's speed and orientation as well as compensating the nonlinearities caused mainly by the hydrodynamic drag [1], [2]. Mid control level is designated to guidance (e.g. path and trajectory following), and high level which is usually in charge of mission control [3], [4]. The main aspect of this paper is the mid level control, specifically, path following. There are many references in literature which deal with path following in marine applications, only some of which are mentioned here [5], [6]. The simplest form of path following is the line-of-sight principle [7] where the vehicle heads towards the target point which is straight in front of it. The problem with this approach

lies in currents which tend to change the predefined path as the vehicle progresses. This problem is resolved in line following algorithms, where a predefined line is followed under any circumstances, i.e. the vessel is always forced to stay on the track. Line following algorithms which have been used on the *Charlie* unmanned catamaran are described in detail in [8], [9], [10]. The problem of 3D line following, which is present in underwater marine applications, introduces some extra issues.

This paper addresses the straight line following problem in 3D for underactuated underwater vehicles. The three dimensional implication complicates the analysis of the problem since a greater number of coupling terms can influence the vehicle behaviour. The main contribution of this paper is the design of 3D line following controllers for underactuated underwater vehicles. The following part of this section introduces mathematical models used to describe underwater vehicles' behaviour along with simplifications used for controller design. Section 2 formulates the problem of 3D line following and Section 3 presents line following mathematical models. The design procedure of proposed 3D line following controllers is given in Section 4, whereas Section 5 presents simulation results. The paper is concluded with Section 6.

2 Problem formulation

2.1 Mathematical model for underwater vehicles

In order to define the full mathematical model of an underwater vehicle the terminology adopted from [11] is used. First of all, two coordinate frames are defined:

- Earth-fixed coordinate system {E} which is steady, immobile coordinate frame. It is usually described with three axis: N (pointing to the north), E (pointing to the east) and D (pointing downward so that NED for a positively oriented coordinate system);
- body-fixed coordinate system {B}, which is usually attached to the centre of gravity (CG) of the vehicle. It is described with three axis x , y and z pointing respectively in the same directions as the NED frame when x and N are aligned.

Table 1 Notation used for marine vehicles
 Tablica 1 Oznake koje se koriste za plovila

DOF	surge	sway	heave	roll	pitch	yaw	defined in
$\boldsymbol{\eta}$	u	v	w	p	q	r	{B}
\mathbf{v}	x	y	z	φ	θ	ψ	{E}
$\boldsymbol{\tau}$	X	Y	Z	K	M	N	{B}

Variables that are included in the mathematical model of marine vehicles are linear and angular velocities, positions and orientations, and forces that excite the vehicle, as listed in Table 1. Surge, sway and heave are defined as motion in the x , y and z axis direction, respectively, while roll, pitch and yaw are defined as rotation about x , y and z axis, respectively.

Earth-fixed coordinate system {E} is used to define vehicle's positions $\boldsymbol{\eta}_1 = [x \ y \ z]^T$ and orientations $\boldsymbol{\eta}_2 = [\varphi \ \theta \ \psi]^T$ forming a six element vector $\boldsymbol{\eta} = [\boldsymbol{\eta}_1^T \ \boldsymbol{\eta}_2^T]^T$. In the same manner, body-fixed coordinate frame is used to define linear velocities $\mathbf{v}_1 = [u \ v \ w]^T$ (surge, sway and heave), and rotational velocities $\mathbf{v}_2 = [p \ q \ r]^T$ (roll, pitch and yaw) forming a six element vector $\mathbf{v} = [\mathbf{v}_1^T \ \mathbf{v}_2^T]^T$. It should be stressed that the speed vector is defined with respect to the water. Motion of the vehicle is achieved by applying external forces and moments. Three forces (each in the direction of one body-fixed frame axis) and three moments (defined as rotation about each body-fixed frame axis) form a six element vector of external forces and moments in the form $\boldsymbol{\tau} = [X \ Y \ Z \ P \ Q \ R]^T$.

Relations between velocities and accelerations of the vehicle and forces that act on it are given with a dynamical model (1) which includes hydrodynamic effects and couplings between motions. In (1) \mathbf{M}_{RB} is diagonal mass and inertia matrix, \mathbf{M}_A is added mass matrix (as a consequence of hydrodynamic effects), \mathbf{C}_{RB} and \mathbf{C}_A are rigid-body and added Coriolis and centripetal matrix (causing the coupling between motions), \mathbf{D} is the damping matrix which is usually approximated by nonlinear diagonal terms that are speed dependant, \mathbf{g} is the matrix of restoring forces which appear due to difference between buoyancy (B) and weight (W) of the submerged vehicle, and $\boldsymbol{\tau}_E$ represents all environmental (stochastic) disturbances that act on the vehicle [11], [12].

$$\underbrace{(\mathbf{M}_{RB} + \mathbf{M}_A)}_{\mathbf{M}} + \underbrace{(\mathbf{C}_{RB}(\mathbf{v}) + \mathbf{C}_A(\mathbf{v}))}_{\mathbf{C}(\mathbf{v})} + \mathbf{D}(\mathbf{v}) + \mathbf{g}(\boldsymbol{\eta}) = \boldsymbol{\tau} + \boldsymbol{\tau}_E \quad (1)$$

The relations between the speeds \mathbf{v} in a body-fixed coordinate frame {B} and first derivative of positions and angles $\boldsymbol{\eta}$ in an Earth-fixed coordinate system {E} are given with a 6DOF kinematic model. A full set of kinematic equations can be found in [11] and is omitted here.

The described model for underwater vehicles is highly nonlinear and coupled, which makes it impractical for control design. Model simplifications that are used in control design make the following assumptions:

- Vessel dynamics is uncoupled, i.e. coupled added mass terms are negligible, center of gravity CG coincides with the origin of the body-fixed coordinate frame {B}, and roll and pitch motion are negligible. This assumption is valid for small remotely operated vehicles which have direct heave DOF control (as is the case in this paper). As a consequence of these simplifications the total Coriolis and centripetal matrix $\mathbf{C}(\mathbf{v})$ vanishes, and restoring forces influence only the heave degree of freedom.
- Drag matrix $\mathbf{D}(\mathbf{v})$ is diagonal and each term can be approximated with a first order speed dependant term.

These simplifications lead to one, generalized, uncoupled, nonlinear dynamic equation that describes surge, sway, heave and yaw degree of freedom separately and it is given with

$$\alpha_v \dot{v}(t) + \beta(v(t)) \cdot v(t) = \tau_{vE} + \tau(t) \quad (2)$$

where v is a single degree of freedom, α_v and $\beta(v)$ are model parameters where $\beta(v) = \beta_v v + \beta_{vv} |v|$, τ is a single degree of freedom excitation force, and $\tau_{vE} = \tau_{NE}$ represents external disturbances. It should be mentioned that for heave DOF τ includes the difference between the weight and the buoyancy.

2.2 Line decomposition

Let the three dimensional space be defined with a conventional NED coordinate frame as it was described before. Let there be an oriented line l given in the NED coordinate frame with the starting point $T_1 = (x_1, y_1, z_1)$, ending point $T_2 = (x_2, y_2, z_2)$ and the vehicle is given with $T_0 = (x_0, y_0, z_0)$ (this is the origin of the {B} frame) as it is shown in Figure 1a). Points T_1 and T_2 define the oriented line l that is to be followed (orientation by convention goes from T_1 to T_2).

Having this in mind, the line l can be decomposed into two components:

- horizontal oriented line l_H uniquely defined as the orthogonal projection of l to the plane $z = z_0$. Since $z = z_0$ is parallel to the $N - E$ plane, the line l_H is uniquely defined with T_1 and angle Γ relative to the $N - D$ plane, given with (3)

$$\Gamma = \arctan \frac{y_2 - y_1}{x_2 - x_1}, \quad (3)$$

- vertical oriented line l_V uniquely defined in the plane Π orthogonal to the $N - E$ plane passing through T_1 . The line l_V is uniquely defined with T_1 and angle χ relative to the $N - E$ plane, given with (4)

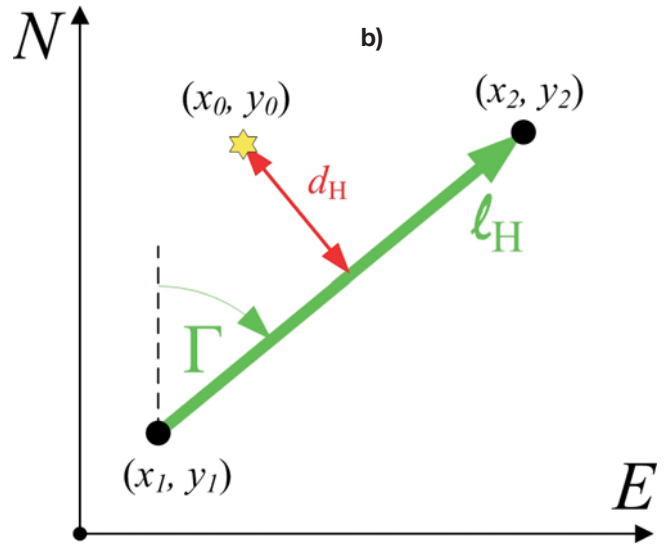
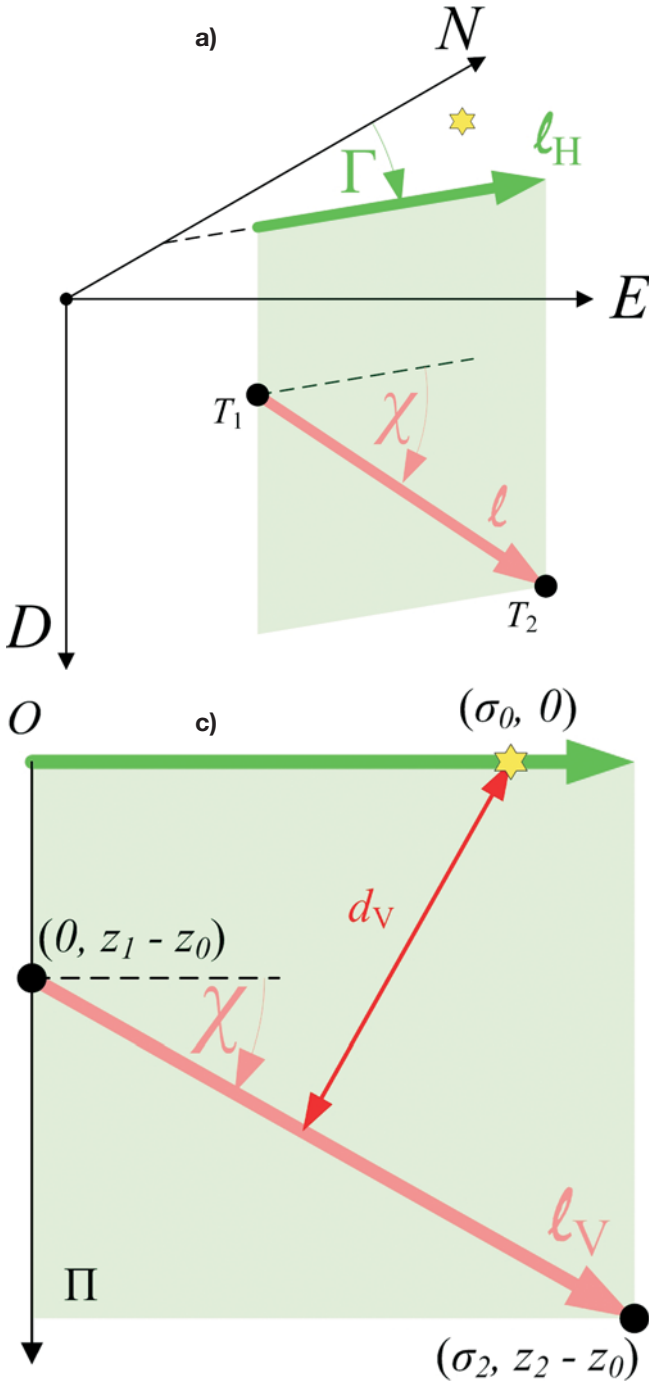
$$\chi = \arctan \frac{z_2 - z_1}{\sqrt{(x_2 - x_1)^2 + (y_2 - y_1)^2}}. \quad (4)$$

This decomposition implies that the 3D line following problem can be observed as following two lines in 2D. The distance of the vehicle to line l_H is then shown in Figure 1b) and can be calculated as the distance of the point (x_0, y_0) to the oriented line given with the points (x_1, y_1) and (x_2, y_2) , given with (5)

$$d_H = \frac{|(x_2 - x_1)(y_1 - y_0) - (x_1 - x_0)(y_2 - y_1)|}{\sqrt{(x_2 - x_1)^2 + (y_2 - y_1)^2}} \quad (5)$$

The vertical distance d_v is observed with regard to the plane Π whose origin O is conveniently placed at the point (x_1, y_1, z_0) . The coordinates of the point T_1 relative to the Π plane are $P_1 = (0, z_1 - z_0)$, and coordinates of the point T_2 relative to the Π plane are $P_2 = (\sigma_2, z_2 - z_1)$ where $\sigma_2 = \sqrt{(y_2 - y_1)^2 + (x_2 - x_1)^2}$. The orthogonal projection of T_0 on the Π plane gives relative coordinates $P_0 = (\sigma_0, 0)$, where $\sigma_0 = \sqrt{\sqrt{(y_0 - y_1)^2 + (x_0 - x_1)^2} - d_H^2}$

Figure 1 a) Oriented line l in the NED frame, and orthogonal projections of all points of interest on the b) $z = z_0$ and c) Π plane
 Slika 1 a) Orijentirani pravac l u NED koordinatnom sustavu i ortogonalne projekcije svih bitnih točaka na b) $z = z_0$ i c) Π ravninu



, as shown in Figure 1c). Now, the vertical distance is calculated as the distance of P_0 to the line described with P_1 and P_2 , and is given with (6)

$$d_v = \frac{-(z_2 - z_1)[(x_2 - x_1)(x_0 - x_1) + (y_2 - y_1)(y_0 - y_1)] - (z_1 - z_0)[(x_2 - x_1)^2 + (y_2 - y_1)^2]}{\sqrt{(x_2 - x_1)^2 + (y_2 - y_1)^2} \sqrt{(x_2 - x_1)^2 + (y_2 - y_1)^2 + (z_2 - z_1)^2}} \quad (6)$$

Now that the crucial parameters for calculating distances with regard to the two lines l_H and l_v are defined, the mathematical model of the vehicle moving relative to the lines can be derived.

3 The line following model

As it was shown in the previous section, 3D line following can be separated into two 2D line following problems. This section presents mathematical models for the l_H and the l_v line following under the assumption that the underwater vehicle is controllable only in surge, heave and yaw degrees of freedom. One such vehicle is a VideoRay ROV (equipped with two horizontal and one vertical thruster) which is used as the case study.

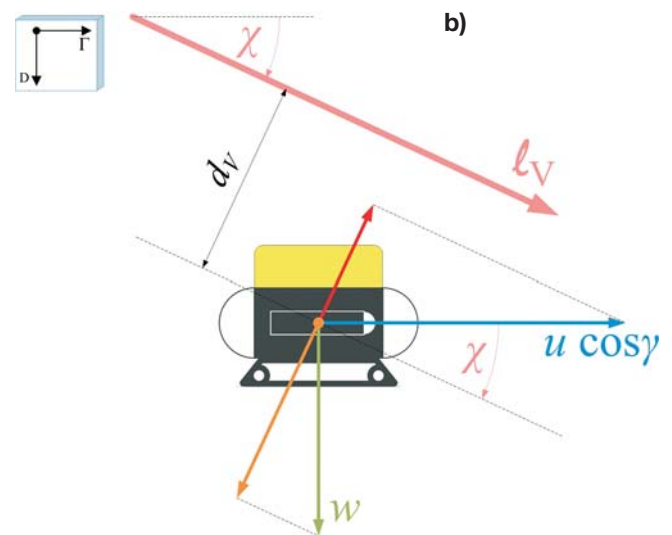
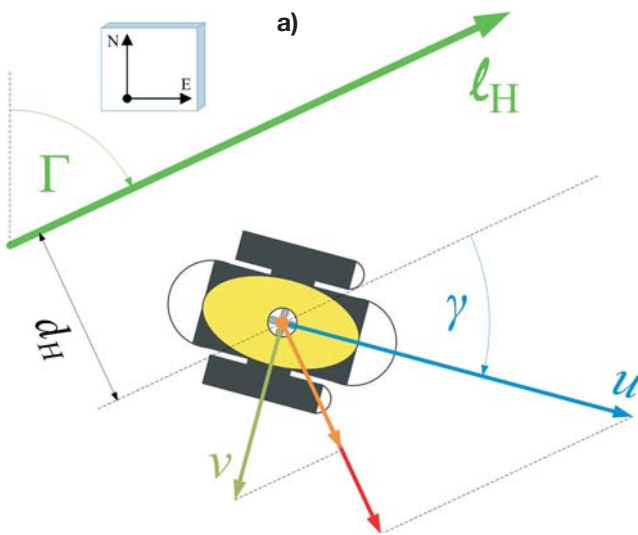


Figure 2 Line following model in a) the $z = z_0$ and b) the Π plane
Slika 2 Model praćenja pravca u a) $z = z_0$ i b) Π ravnini

3.1 The l_H line following model

The scheme for following the oriented line l_H is shown in Figure 2a) and the equations follow:

$$\dot{d}_H = u \sin \gamma + v \cos \gamma + \xi_H \quad (7)$$

$$\dot{\gamma} = r \quad (8)$$

$$\dot{r} = -\frac{\beta(r)}{\alpha_r} r + \frac{1}{\alpha_r} N \quad (9)$$

The distance d_H with regard to the line l_H changes due to surge u and sway speed v . In the observed ROV, sway speed cannot be controlled. However, by changing the attack angle $\gamma = \psi - \Gamma$, the vehicle can be forced to approach the line. Therefore, the term $u \sin \gamma$ in (7) is the only controllable term, unlike $v \cos \gamma$ which appears either due to external disturbance acting in the sway direction, or due to coupling between the motions. Parameter ξ_H presents any additional disturbance (horizontal current perpendicular to the target line) and unmodelled dynamics in the system. The yaw dynamics is given with (9) according to (2). A simplification which can be done in (7) is to assume that the approach angle γ is small enough to assume that $\sin \gamma \approx \gamma$. This assumption makes the controller design simpler since the system, at least at the kinematic level, is linearized.

3.2 The l_v line following model

The scheme for following the oriented line l_v is shown in Figure 2b) and the equations follow (B and W have been defined before as buoyancy and weight of the vehicle, respectively). The figure shows the situation when the ROV is aligned with l_H ($\Gamma = \psi$) which need not be the case. The misalignment is included in the effect of the surge speed.

$$\dot{d}_v = w \cos \chi - u \cos \gamma \sin \chi + \xi_v \quad (10)$$

$$\dot{w} = -\frac{\beta(w)}{\alpha_w} w + \frac{1}{\alpha_w} (Z + W - B) \quad (11)$$

The distance with regard to l_v changes due to surge u and heave speed w , and the equation is given with (10). Parameter ξ_v presents any external disturbance and unmodelled dynamics in the system. Heave dynamics is given with (11), where the influence of the discrepancy between buoyancy and weight is excluded from the heave force Z .

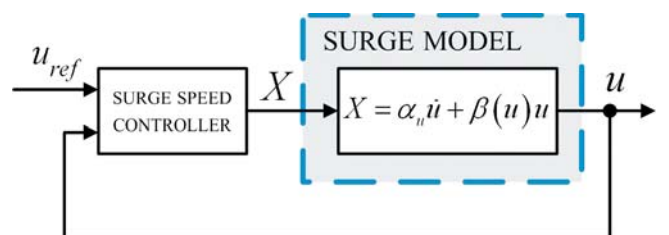
4 Line following controller design

Once the mathematical model of underwater vehicles and line following models in the two planes have been presented, the line following controllers for both lines can be developed independently. The independence in design comes from the fact that the assumed, simplified single DOF model is uncoupled and given with (2) for each DOF.

4.1 Surge speed control

In order to make the task of designing line following controllers in a simpler manner, the demand is to have a constant surge speed during the experiment. If the speed is controlled in open loop, the couplings between the motions might reduce the speed

Figure 3 Surge speed control loop
Slika 3 Petlja upravljanja unaprijednom brzinom



during complex manoeuvres. This is the main motivation why surge speed controller shown in Figure 3 is designed.

The surge speed u controller which is proposed in this paper is a I-P controller modified to compensate the process' nonlinearity, if it exists, and it is given with (12) [1]. This controller ensures zero steady state error and compensation of external disturbances.

$$X = K_{Iu} \int_0^t (u_{ref} - u) dt - K_{Pu} u + \beta(u)u \quad (12)$$

The choice of the controllers that feed separately derivative (or proportional) channels directly from the output instead from the output of the comparator is quite common in marine applications [13]. Since abrupt changes on actuators are not permitted (due to wearout), the control difference signal should not be fed through the derivation or even proportional channel. Therefore, with this type of controller, if step changes to desired surge speed u_{ref} are required, the controller output is smooth, not causing any stress on the actuators.

The controller parameters are tuned using a model based procedure. The closed loop transfer function, when controller (12) is used, is given with

$$\frac{u}{u_{ref}} = \frac{1}{\frac{\tilde{\alpha}_u K_{Iu}}{a_{2u}} s^2 + \frac{K_{Pu} K_{Iu}}{a_{1u}} s + 1} \quad (13)$$

where a_{2u} and a_{1u} are the desired, predefined, closed loop transfer function parameters. The controller parameters are then given with (14).

$$\begin{aligned} K_{Pu} &= \frac{a_{1u}}{a_{2u}} \\ K_{Iu} &= \frac{1}{a_{2u}} \tilde{\alpha}_u \end{aligned} \quad (14)$$

The most appropriate choice for the desired closed loop dynamics would be a Butterworth or a Bessel filter with a characteristic frequency chosen according to the vehicles performance capabilities (speed of response) [14].

4.2 The l_H line following controller

There are a number of approaches which can be used for line following control in horizontal plane [10], [15]. One such approach, which is used in this paper is the direct actuator control.

This method implies the design of two controllers: inner yaw rate controller and outer line following controller, as it is shown in Figure 4. This approach is advised if the vehicle control system allows direct actuator commands (i.e. if inner closed loop controllers can be tuned) and if yaw rate measurements or estimates are available. It should be mentioned that direct actuator control is not always possible (or available), in case of which other strategies are employed [10].

The l_H line following controller gives the reference yaw rate r_{ref} as output. The yaw rate controller is designed using the same control algorithm as for the surge controller and it is given with (15). This controller ensures zero steady state error and compensation of external disturbances.

$$N = K_{Ir} \int_0^t (r_{ref} - r) dt - K_{Pr} r + \tilde{\beta}(r)r \quad (15)$$

Under the assumption that the yaw rate closed loop is $\frac{r_{ref}}{r}$, the following transfer function when the line following controller is not present can be written:

$$\frac{d}{r_{ref}} = \frac{u}{s^2} \frac{r}{r_{ref}} \quad (16)$$

The line following controller can be chosen as PD type which compensates for external disturbances and ensures zero steady state error even though integral action does not exist. The reason for this is that the integral action is inherent to the process as it is shown in Figure 4. The proposed controller is given with

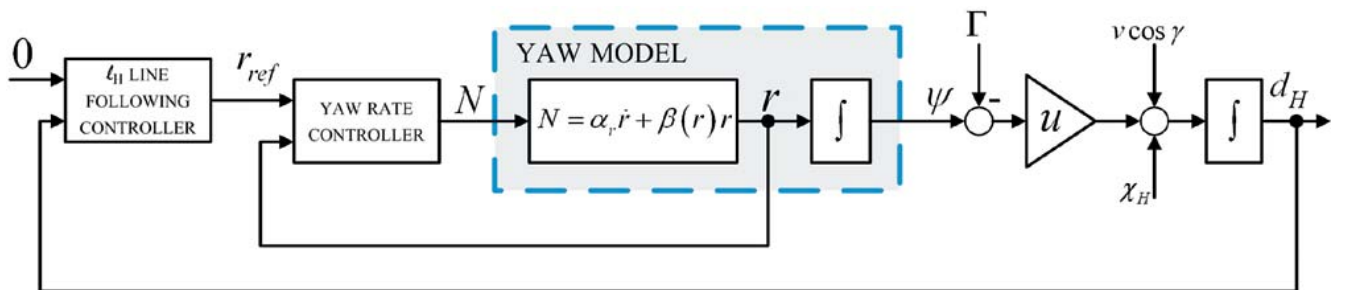
$$r_{ref} = K_{ph} (d_{H,ref} - d_H) + K_{Dh} \frac{d}{dt} (d_{H,ref} - d_H) \quad (17)$$

which yields the complete closed loop transfer function given with (18) where a_{4h} , a_{3h} , a_{2h} and a_{1h} are desired line following closed loop transfer function parameters (h stands for horizontal plane). The controller is designed for small angles of attack, where the assumption $\sin \gamma \approx \gamma$ is valid.

$$\frac{d_h}{d_{h,ref}} = \frac{1 + K_{Dh} K_{ph} s}{\frac{\alpha_r u K_{Ir} K_{ph}}{a_{4h}} s^4 + \frac{K_{Pr} u K_{Ir} K_{ph}}{a_{3h}} s^3 + \frac{1uK_{ph}}{a_{2h}} s^2 + \frac{K_{Dh} K_{ph}}{a_{1h}} s + 1} \quad (18)$$

From (18), the line following controller parameters can be calculated using (19). From here it is evident that by setting the desired line following closed loop dynamics, the inner closed loop parameters are set automatically.

Figure 4 The l_H line following closed loop (the direct actuator control approach)
Slika 4 Zatvoreni krug praćenja pravca l_H (pristup izravnog upravljanja izvršnim uređajem)



$$\begin{aligned}
 K_{lr} &= \frac{a_{2h}}{a_{4h}} \alpha_r, & K_{Pr} &= \frac{a_{3h}}{a_{4h}} \alpha_r \\
 K_{ph} &= \frac{1}{ua_{2h}}, & K_{Dh} &= \frac{a_{1h}}{ua_{2h}}
 \end{aligned}
 \tag{19}$$

4.2.1 Monotonous approach

If the line that the vehicle should approach is too far from the current vessel position, the vessel might start performing a spiral movement towards the line, or even worse it may start rotating at the smallest possible turn radius given the reference surge speed. This section describes the procedure given in [16] which prevents this effect from happening in the case of the previously described direct actuator control.

If the line following controller is given with (17) where the assumption is made that $d_{ref} = 0$, and if d is large enough, the proportional part may result in r_{ref} so large that the vessel starts

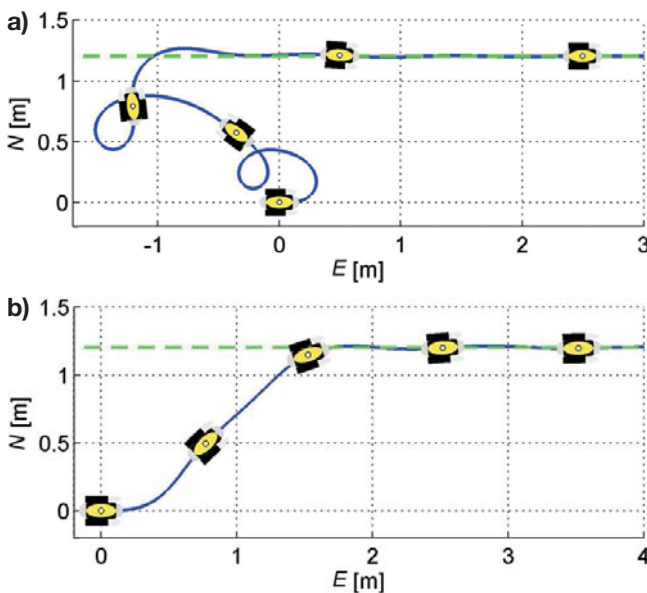


Figure 5 a) The spiral path towards the line and b) elimination of this effect when controller modification (21) is applied
 Slika 5 a) Spiralna putanja prema liniji i b) uklanjanje ovog efekta uz primjenjenu modifikaciju (21) na regulatoru

rotating or moving spirally towards the line as it is shown in Figure 5. In this case, the distance to the path is not monotonously decreasing and this presents an unacceptable behaviour. The simulation in Figure 5 was conducted with line orientation $\Gamma = 90^\circ$, initial vessel heading $\psi(0) = 90^\circ$ and initial distance from the line $d(0) = 1.2$ m.

This problem can be heuristically addressed if the reference yaw rate is demanded to be zero, i.e. $r_{ref} = 0$ when the rotation occurs. By combining this demand with (17) a limitation to the maximal allowed distance when the line following controller can be turned on is given with (20) where the maximum absolute value of $v \cos \gamma + \xi_H$ is denoted with $\bar{\xi}$ and $\bar{\gamma}$ is the maximum allowed approach angle to the line.

$$|d| < \frac{K_{ph}}{K_{Dh}} (u \sin \bar{\gamma} - \bar{\xi}) = \bar{d}.
 \tag{20}$$

It should be mentioned that this saturation has variable saturation limits if true surge speed is applied (whereas one could just use $u = u_{ref}$), and true sway speed measurements are available.

Since $|d| > 0$ and $\sin \beta < 1$, the trivial solution $\bar{v} < u_r$ is embedded. In other words, limiting the value d in (17), the heuristic line following control law is given with

$$r_{ref} = -K_{pd} \text{sat}(d, -\bar{d}, \bar{d}) - K_{Dd} \dot{d}
 \tag{21}$$

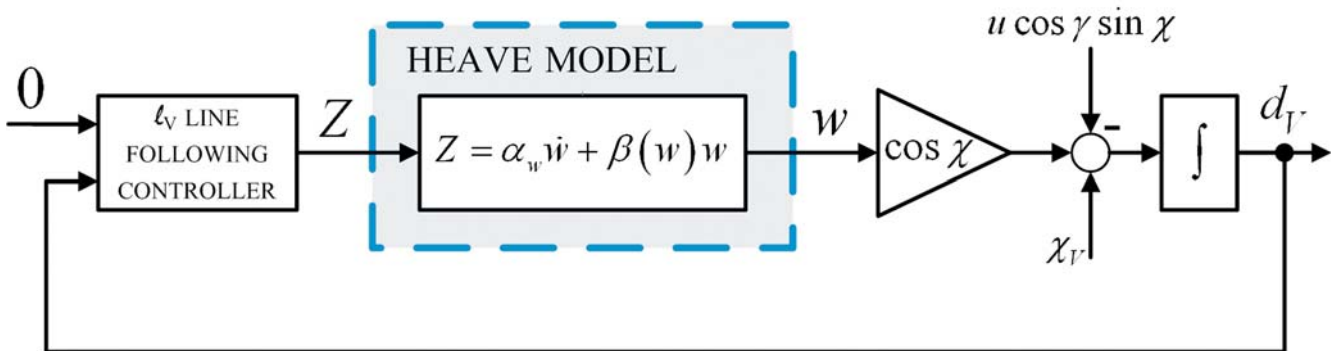
which forces the vessel to approach the target line for large values of $|d|$ with approach angle γ such that $r_{ref} = 0$. The function $\text{sat}(d, -\bar{d}, \bar{d})$ is the saturation of the value d to the upper limit \bar{d} and lower limit. The Lyapunov proof of stability of this control system can be found in [16]. When control law (21) is used, the path of the vessel is shown in Figure 5b) from where it is obvious that the approach to the desired line is monotonous at a predefined approach angle $\bar{\gamma} = 45^\circ$. The line orientation and initial conditions are the same as in the case shown in Figure 5a).

4.3 The l_v line following controller

The proposed control structure for the l_v line following controller is shown in Figure 6.

The controller output is heave force and its algorithm is of I-PD type given with (22). This controller compensates for external disturbances and ensures zero steady state error. It should be mentioned that this structure is the same as the classical PID

Figure 6 The l_v line following closed loop
 Slika 6 Zatvoreni krug praćenja pravca l_v



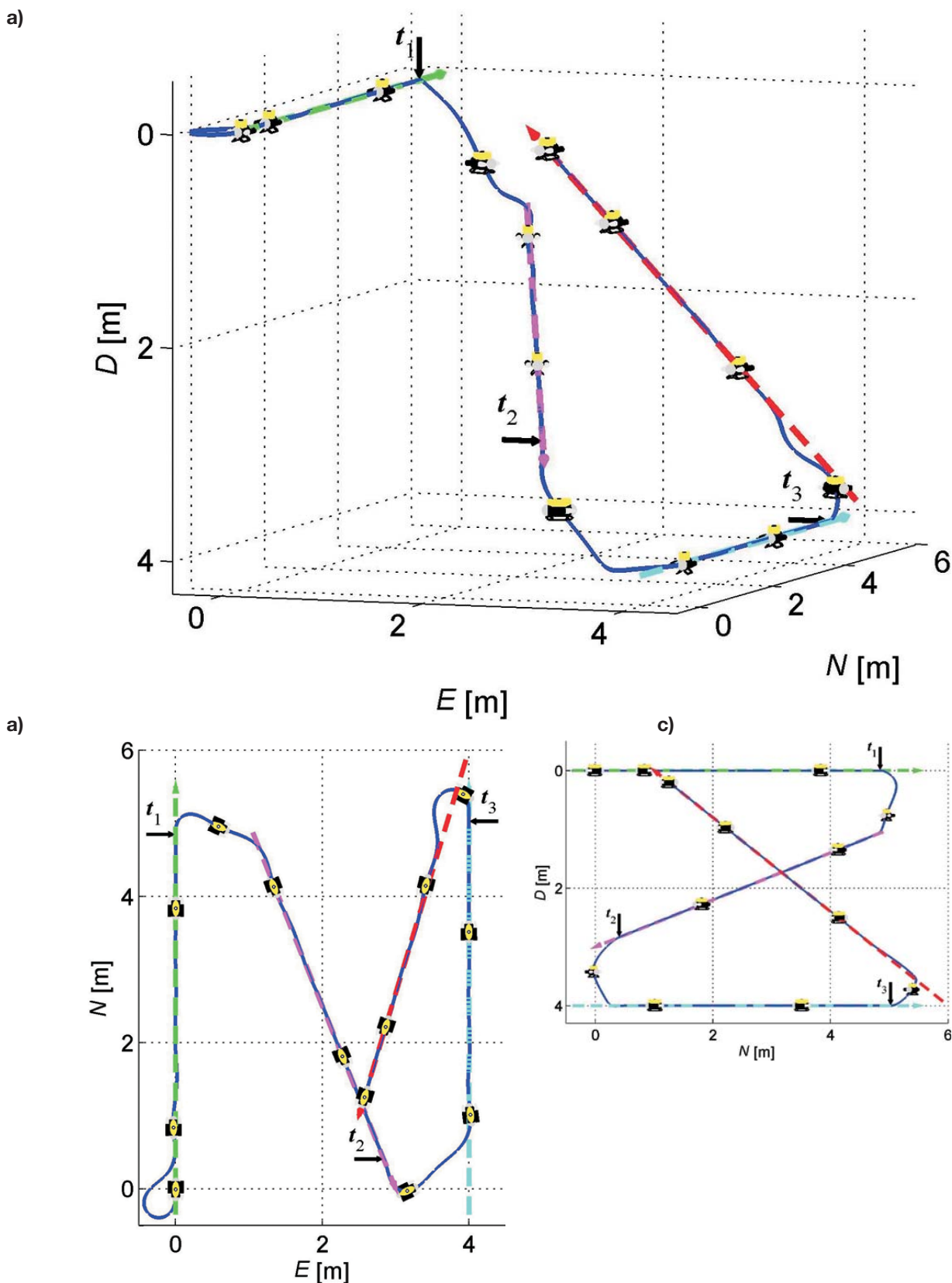


Figure 7 Path of the underwater vehicle in a) the *NED* frame, b) the *N - E* plane, and c) the *N - D* frame
 Slika 7 Putanja ronilice u a) *NED* koordinatnom sustavu, b) *N - E* ravnini i c) *N - D* ravnini

controller if $d_{v,ref} = 0$ which is the case if line following is required.

$$Z = K_{Iv} \int_0^t (d_{v,ref} - d_v) dt - K_{Pv} d_v - \frac{d}{dt} d_v \quad (22)$$

The closed loop form is then given with (23) where a_{3v} , a_{2v} and a_{1v} are desired line following closed loop transfer function parameters (v stands for vertical plane).

$$\frac{d_v}{d_{v,ref}} = \frac{1}{\frac{\alpha_w K_{Iv} \cos \chi s^3 + \beta_w + K_{Dv} \cos \chi K_{Iv} \cos \chi s^2 + K_{Pv} K_{Iv} s + 1}{a_{3v} a_{2v} a_{1v}}} \quad (23)$$

From here the controller parameters follow:

$$K_{Iv} = \frac{\alpha_w}{\cos \chi} \frac{1}{a_{v3}}, \quad K_{Pv} = \frac{\alpha_w a_{v1}}{\cos \chi a_{v3}}, \quad K_{Dv} = \frac{\alpha_w a_{v2}}{\cos \chi a_{v3}} - \frac{\beta_w}{\cos \chi} \quad (24)$$

It should again be mentioned that the choice of the desired closed loop function parameters depends on the feasible dynamics of the underwater vehicle.

5 Results

The simulation results which are presented here were obtained on a simulation model of a VideoRay ROV. The underwater vehicle weighs about 4.5 kg and its model parameters were taken from [17] and [18]. The model which was used to perform the simulations was fully coupled. This way the assumption on the controller design by using the uncoupled equations were tested. In addition to this, the saturations on exerted thrusts and moments were implemented, which contributed to the real vehicle behaviour. It should be mentioned that saturations necessarily include the introduction of the antiwindup mechanisms in the controllers [19].

The simulation case study which is presented here includes the vehicle to follow four lines. The switching between the lines is time based. The switching times together with two points T_1 and T_2 that describe the 3D line l are given in Table 2. It should be mentioned that the switching can be position based: when the vehicle approaches the final point T_2 , the following line is set to be followed.

Table 2 **Switching times and the l line parameters during the simulated mission**
 Tablica 2 **Trenutci zadavanja sljedećeg pravca i parametri pravca l tijekom simulirane misije**

SWITCH TIME	$T_1 (x_1, y_1, z_1)$	$T_2 (x_2, y_2, z_2)$
$t_0 = 0$ s	(0, 0, 0)	(5, 0, 0)
$t_1 = 60$ s	(5, 1, 1)	(0, 3, 3)
$t_2 = 120$ s	(0, 4, 4)	(5, 4, 4)
$t_3 = 180$ s	(6, 4, 4)	(1, 2.5, 0)

Figure 7a) gives the 3D representation in the NED frame of the vehicle path (blue solid line) and the lines which are to be followed. The reference surge speed was held to 0.1 m/s through the whole experiment. Switching times are clearly indicated. The same path is given as orthogonal projection on the $N - E$ and $N - D$ planes in Figure 7b) and Figure 7c) respectively. These results

show that the proposed control structure for line following can be applied in practice.

It is clearly seen how the vehicle approaches with a constant approach angle to the line when the distance to the line is substantial. Probably the most complex manoeuvre in the path, is just after $t = t_3$ time instance when the underwater vehicle is supposed to change its direction by almost 180° , emerge towards the surface and maintain the constant forward speed. The coupling effects are significant, but the convergence to the line is well performed.

The videos of the same simulation experiment which may be more descriptive for the reader, can be found online at http://lapost.fer.hr/nmiskovic/line_following_3D/.

6 Conclusion

In this paper a problem of following a 3D line was formulated by separating the line into a horizontal and a vertical component. Further on, the 3D line following problem was investigated from the perspective of an underwater underactuated vehicle. The proposed methodology for line following is based on developing a surge controller for keeping the constant surge speed during the execution of the experiment (otherwise the speed would change significantly due to coupling effects), a line following controller in the horizontal plane which generates reference yaw rate for the low level yaw rate controller, and a line following controller in the vertical plane which generates directly desired heave thrust. The controllers were designed on the assumption that the vehicles' dynamics was uncoupled, and were tested on a coupled model. The results have shown that the proposed procedure is applicable for 3D line following problem in underwater marine vehicles whose dynamics is nonlinear and coupled.

Acknowledgments

The work was carried out in the framework of a Coordination and Support Action type of project supported by the European Commission under the Seventh Framework Programme "CURE - Developing Croatian Underwater Robotics Research Potential" SP-4 Capacities (call FP7-REGPOT-2008-1) under Grant Agreement Number: 229553, and in the framework of the research project "RoboMarSec - Underwater robotics in sub-sea protection and maritime security" supported by the Ministry of Science, Education and Sports of the Republic of Croatia (Project No.036-0362975-2999).

References

- [1] MIŠKOVIĆ, N., VUKIĆ, Z., OMERDIĆ, E.: "Control of UUVs Based upon Mathematical Models Obtained from Self-Oscillations Experiments", Proc. of IFAC Navigation Guidance Control of Underwater Vehicles Conference, 2(1), Lakeside Hotel, Ireland, 2008.
- [2] MIŠKOVIĆ, N., VUKIĆ, Z., BARISIC, M., TOVORNIK B.: "Autotuning autopilots for micro-ROVs", Proc. of the 14th Mediterranean Conference on Control and Applications, pp.1-6, 2006.
- [3] BIBULI, M., BRUZZONE, G., CACCIA, M.: "Mission Control for Unmanned Underwater Vehicles: functional requirements and basic system design", Proc. of IFAC

- Navigation Guidance Control of Underwater Vehicles Conference, Lakeside Hotel, Ireland, 2008.
- [4] BIBULI, M., BONO, R., BRUZZONE, G., CACCIA, M.: "Event handling towards mission control for unmanned marine vehicles", Proc. of IFAC Conference on Control Applications in Marine Systems, Bol, Croatia, 2007.
- [5] BREIVIK, M., FOSSEN, T.I.: "Guidance Laws for Planar Motion Control", Proc. of 47th IEEE Conference on Decision and Control, p. 570-577, Cancun, Mexico, 2008.
- [6] BREIVIK, M., FOSSEN, T.I.: "Path following for marine surface vessels", Proc. of Oceans 2004, p. 2282-2289, Kobe, Japan, 2004.
- [7] FOSSEN, T. I., BREIVIK, M., SKJEME, R.: "Line-of-sight path following of underactuated marine craft", Proceedings of the 61st IFAC MCMC Conference, Cimno, Spain, 2003.
- [8] BIBULI, M., CACCIA, M., LAPIERRE, L.: "Path-following algorithms and experiments for an autonomous surface vehicle", Proc. of IFAC Conference on Control Applications in Marine Systems, Bol, Croatia, 2007.
- [9] BIBULI, M., BRUZZONE, G., CACCIA, M., INDIVERI G., ZIZZARI, A.A.: "Line Following Guidance Control: Application to the Charlie Unmanned Surface Vehicle", Proc. of IEEE/RSJ 2008 International Conference on Intelligent Robots and Systems, Nice, France, 2008.
- [10] MISKOVIC, N., BIBULI, M., BRUZZONE, G., CACCIA, M., VUKIĆ, Z.: "Tuning Marine Vehicles' Guidance Controllers through Self-Oscillation Experiments", Proceedings of the MCMC'09 Conference, Guarujá, Brasil, 2009.
- [11] FOSSEN, T.I.: "Guidance and Control of Ocean Vehicles", John Wiley & Sons, New York, USA, 1994.
- [12] OMERDIC, E.: "Thruster fault diagnosis and accommodation for overactuated open-frame underwater vehicles", PhD thesis, University of Wales College, Newport, United Kingdom, 2002.
- [13] VUKIĆ, Z., KULJAČA, Lj.: "Automatic Control - Analysis of Linear Systems", Kigen, Zagreb, 2005, (in Croatian).
- [14] MISKOVIC, N., VUKIC, Z., BIBULI, M., CACCIA, M., BRUZZONE, G.: "Marine vehicles' line following controller tuning through self-oscillation experiments", 17th Mediterranean Conference on Control and Automation, pp.916-921, Thessaloniki, Greece, 2009.
- [15] CACCIA, M., INDIVERI, G., VERUGGIO, G.: "Modelling and identification of open-frame variable configuration unmanned underwater vehicles", IEEE Journal of Oceanic Engineering, 25(2), p. 227-240, 2000.
- [16] CACCIA, M., BIBULI, M., BONO, R., BRUZZONE, G.: "Basic navigation, guidance and control of an Unmanned Surface Vehicle", Autonomous Robots 25(2008)4, p. 349-365, Springer Science+Business Media.
- [17] WANG, W., CLARK, C.M.: "Modeling and Simulation of the VideoRay Pro III Underwater Vehicle", OCEANS 2006 - Asia Pacific, p. 1-7, 2006.
- [18] STIPANOV, M., MISKOVIC, N., VUKIC, Z. AND BARI-SIC, M.: "ROV autonomization - yaw identification and Automarine module architecture", Proc. of the CAMS'07 Conference, 2007.
- [19] CHOI, J.-W., LEE, S.-C.: "Antiwindup Strategy for PI-Type Speed Controller", IEEE Transactions on Industrial Electronics, 56(2009)6, p. 2039-2046.